# Flexible Strain and Temperature Sensing NFC Tag for Smart Food Packaging Applications

Pablo Escobedo, Mitradip Bhattacharjee, *Member, IEEE*, Fatemeh Nikbakhtnasrabadi, *Graduate Student Member, IEEE*, and Ravinder Dahiya, *Fellow, IEEE*

***Abstract*—This paper presents a smart sensor patch with flexible strain sensor and a printed temperature sensor integrated with a Near Field Communication (NFC) tag to detect strain or temperature in a semi-quantitative way. The strain sensor is fabricated using conductive polymer poly (3,4-ethylenedioxythiophene) polystyrene sulfonate (PEDOT: PSS) in a polymer Polydimethylsiloxane microchannel. The temperature sensor is fabricated by printing silver electrodes and PEDOT:PSS on a flexible polyvinyl chloride (PVC) substrate. A custom-developed battery-less NFC tag with an LED indicator is used to visually detect the strain or temperature by modulating the LED light intensity. The LED shows maximum brightness for relaxed or no strain condition, and also in the case of maximum temperature. In contrast, the LED is virtually off for the maximum strain condition and for room temperature. Both these could be related to food spoilage. Swollen food packages can be detected with the strain sensor, serving as beacons of microbial contamination. Temperature deviations can result in the growth or survival of food-spoilage bacteria. Based on this, the potential application of the sensor system for smart food packaging is presented.**

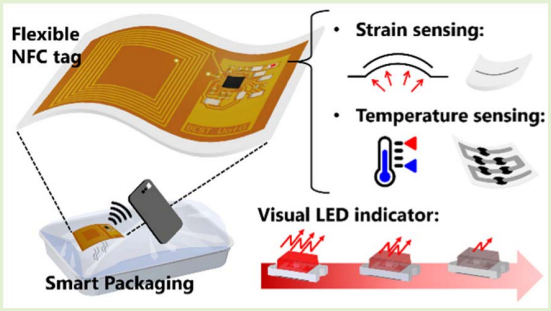


***Index Terms*—Flexible electronics, NFC tag, strain sensor, smart food packaging, temperature sensor, wireless communication.**

## I. Introduction

TECHNOLOGICAL advances in smart sensors and wireless interfaces are bringing the digital and physical worlds closer together through remote monitoring of a wide variety of parameters, finding application in the fields of agriculture, healthcare, etc. [1], [2] These advances have also enabled the use of robots during various stages of agriculture or farm produce, such as fruit picking and packaging [3]–[5]. To this end, several physical and chemical sensors have been developed to gather information about temperature [6]–[8], pressure [9]–[11], strain [12]–[14], humidity [15], [16], pH [17], [18], volatile organic compounds (VOCs) [19], etc. Further, the advances in nanotechnology and Printed Electronics (PE) have unlocked interesting avenues for sensing using various functional and degradable materials in applications such as smart labels for food, pharmaceutical and wearables [20]–[24]. The wireless acquisition of the data from the sensors in most of smart labels is achieved through technologies such as Radiofrequency Identification (RFID), Near Field Communication (NFC) or Bluetooth. Lightweight, flexibility, security, and low-power consumption are desired properties for these wireless sensor systems. In particular, the use of RFID technology makes it possible to develop battery-free sensor systems [25] and their use in sensing tags for smart food packaging is particularly attractive [26]. Such tags or smart labels could help mitigate the food spoilage by alerting the consumer or food provider when a product is likely to be or has been compromised [27], [28]. These technologies are also much needed to address hunger

Manuscript received April 4, 2021; accepted July 23, 2021. Date of publication July 30, 2021; date of current version November 30, 2021. This work was supported in part by the Engineering and Physical Sciences Research Council (EPSRC) through the Engineering Fellowship for Growth—neuPRINTSKIN under Grant EP/R029644/1, in part by the North West Centre for Advanced Manufacturing (NWCAM) Project through the European Union's INTERREG VA Programme under Grant H2020-Intereg-IVA5055, and in part by the Special EU Programmes Body (SEUPB). The associate editor coordinating the review of this article and approving it for publication was Dr. Luigi Occhipinti. *(Pablo Escobedo and Mitradip Bhattacharjee contributed equally to the work.) (Corresponding author: Ravinder Dahiya.)*

Pablo Escobedo, Fatemeh Nikbakhtnasrabadi, and Ravinder Dahiya are with the Bendable Electronics and Sensing Technologies (BEST) Group, James Watt School of Engineering, University of Glasgow, Glasgow, Scotland G12 8QQ, U.K. (e-mail: Ravinder.Dahiya@glasgow.ac.uk).

Mitradip Bhattacharjee is with the Bendable Electronics and Sensing Technologies (BEST) Group, James Watt School of Engineering, University of Glasgow, Glasgow, Scotland G12 8QQ, U.K., and also with the Department of Electrical Engineering and Computer Science, Indian Institute of Science Education and Research (IISER), Bhopal, Madhya Pradesh 462066, India.

Digital Object Identifier 10.1109/JSEN.2021.3100876

related global challenges. For example, United Nation's Food and Agriculture Organization (FAO) estimates that roughly one-third of all food produced for human consumption is lost or wasted worldwide [29]. This corresponds to 1.3 billion tonnes of food per year. Much of this wasted food is still safe to eat, but consumers throw it away because it is close to or beyond its printed expiration date. In some cases, smart labels could be useful to provide better estimates of the packaged food quality.

Addressing this need, we present herein a smart tag with potential application for smart food packaging. The tag comprises of a flexible sensors (either a microchannel-based flexible strain sensor, or a printed temperature sensor) and a light-emitting diode (LED) indicator to detect dynamic strain or temperature in a semi-quantitative and visual way (Fig. 1). Both sensors are based on the resistive sensing principle. The visual LED indicator was connected in series with either of the sensors. The strain sensor uses conductive polymer poly (3,4-ethylenedioxythiophene) polystyrene sulfonate (PEDOT:PSS) as the active material in a microchannel made from flexible and transparent Polydimethylsiloxane (PDMS) polymer. The temperature sensor consists of silver electrodes and PEDOT:PSS printed on a flexible polyvinyl chloride (PVC) substrate. A custom planar coil antenna was designed and fabricated to achieve battery-less operation by powering the tag using an NFC reader. This paper extends our work presented during IEEE FLEPS 2020 conference [30]. In addition to the strain sensor reported earlier, this paper also includes the temperature sensor, detailed characterisation of both sensors and the potential applicability of the sensor system for smart food packaging as a proof of concept.

This paper is organised as follows: The concept of the developed smart tag is described in Section II, along with a brief state of the art related to the key components of the tag. The materials and methods used are described in Section III. A detailed discussion of the results is presented in Section IV. Finally, the key outcomes are summarised in Section V, along with the future outlook.

## II. Concept and State of the Art

In most food packages, the presence of undesired gases could indicate the loss of quality and shelf-life of the food, as they originate from the oxidation of the content or the microbial growth [31]. While spoilage can take many forms, inflated or swollen food packages serve as the beacon of microbial contamination. This is known as Blown Pack Spoilage (BPS) [32]–[34]. In vacuum-packaged meat, BPS is mainly caused by *Clostridium estertheticum* and it is characterised by the production of large volumes of gas (mainly carbon dioxide, $CO_2$), which result in severe distention of the packaging [35], [36]. Therefore, swelling might be an initial sign of harmful bacterial activity within the food package, leading to discoloration, nutritional loss, and final spoilage [37]. In the literature, the vast majority of food monitoring methods are based on measuring the gas concentrations emitted from food in a container, thus utilizing chemical sensors [23], [27]. In this case, our presented smart sensing tag detects strain and temperature to monitor packaged

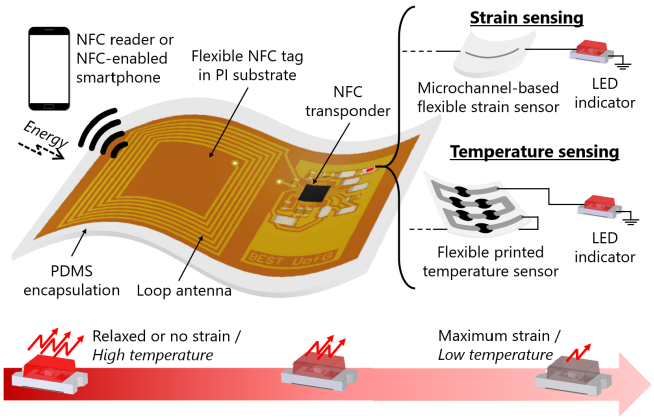


Fig. 1. Overview of the smart tag with NFC-based sensing system.

food quality. The works reported in this direction do not have either the sensing arrangement for physical parameters monitoring or the electronic system to monitor or display the condition, as shown in Table I [38]–[43]. In the particular case of RFID/NFC tags for temperature/strain sensing [44]–[46], the use of physical sensors to detect the distention of the packaging as a result of BPS is lacking in the current state of the art. In this context, the bulge in a food package can be detected using an appropriate strain sensor integrated with it. Temperature is another crucial factor in determining the shelf-life of food products [47]. Temperature alterations can provoke the growth or survival of food-spoilage microorganisms and bacteria [48]. Although there can be several other parameters (e.g., chemical parameters such as pH) to evaluate the food quality, temperature and strain are two critical physical parameters that can indirectly help to evaluate the quality of food. Therefore, the sensor tag presented here (Fig. 1) consists of strain and temperature sensors only.

Strain sensors are devices that generally produce an electrical signal in response to the mechanical deformation or strain of the surface to which they are bonded. Among various transduction mechanisms (e.g., piezoelectricity, triboelectricity, optical methods, etc.), strain sensors commonly use resistive and capacitive mechanism [49], [50]. Conventional strain sensors are stiff and therefore not adequate to detect small deformations in food packages [51], but this issue can be addressed by using flexible strain sensors [52]. These sensors can be fabricated using a variety of approaches such as printing methods [53], [54], conductive fabrics [20], [55] or polymer-based materials [8], [56]. Flexible, light, and conformable substrates such as polyamide (PI), polyethylene terephthalate (PET), polyethylene naphtholate (PEN), etc. that are used in different fields such as robotics [5], [57], health and environmental monitoring [17], [58] are also useful for food packaging. The choice of the flexible substrate ultimately depends on the specific application. For example, PVC has been reported in the literature for food packaging applications because of its thermal stability.

Regarding temperature sensors, the conventional ones are usually made of semiconductors [59], carbon derivatives [8], [60], [61] and temperature-sensitive materials.

TABLE I
COMPARISON WITH SIMILAR SENSOR TAGS FOR PACKAGED FOOD QUALITY

| Sensed Parameters | Sensing Method | Electronic System | Wireless Connectivity | Ref |
|---|---|---|---|---|
| Temperature | Redox Reaction | No | No | [38] |
| $CO_2$ | Dye | No | No | [39] |
| $O_2$ | Redox dye | No | No | [40] |
| Humidity | Dielectric constant change | Yes | RFID | [41] |
| Humidity | Dielectric constant change | Yes | RFID | [42] |
| Bacteria | Antibody interaction | No | No | [43] |
| Air pressure | Commercial pressure sensor | Yes | NFC | [44] |
| Temperature/ Strain | Resistive response | Yes | NFC | This work |

Conductive polymers have also attracted significant attention for temperature sensing, owing to their ease of processing and excellent electrical properties [62]. However, polymers also suffer from low stability at high temperature. In this regard, PEDOT:PSS is attractive as it is one of the most stable organic conductive polymers and it exhibits electrical properties similar to a metal or semiconductor [63], [64]. Therefore, this material is suitable for the fabrication of temperature sensors on flexible substrates and can operate over high-temperature ranges. For this reason, PEDOT:PSS is used in this work as the active sensing material for both temperature and strain sensors.

The response of the sensors at different temperature/strain conditions can be quantified and displayed using standard seven segment displays. However, for food packaging applications the exact values of temperature or strain are not always needed, as often the goal is only to identify if the food is stale or not. Given this scenario, a simple indicator to warn only when the packed food is stale can be more cost-effective. For this reason, the smart tag presented here includes an LED connected in series with the developed resistive sensors (Fig. 1). The varying resistance of sensors modulates the light intensity of the LED indicator, thus allowing the user to detect the state of food in a visual way.

The wireless communication is another important aspect of smart tags. In this regard, RFID has emerged as the workhorse technology. Depending on the frequency range of operation, RFID systems classified as low frequency (LF), high frequency (HF), and ultra-high frequency (UHF) systems. Among them, UHF RFID systems (860 – 960 MHz) have the greatest read range (3 – 15 m) and the highest reading speed, but they require the use of specialised equipment and reader antennas [65]. HF systems (3 – 30 MHz) usually have a read range of a few centimetres up to about a meter and make use of magnetic coupling to communicate between the HF tag and the RFID reader. A specialized subset of HF band is the NFC, which operates at a single frequency (13.56 MHz) and is a global communication protocol approved by the International Organization of Standardization (ISO). It mainly focuses on secure identification applications [66]. A key advantage of NFC tags over other RFID systems lies in their ability to be read by NFC-enabled smartphones, making this technology within the reach of any individual user [67], [68]. For this reason, NFC sensing tags have gained widespread popularity in countless applications such as wearable health, smart packaging, and modified atmosphere packaging (MAP) for food monitoring [27], [46], [69]. In this work, an NFC antenna has been designed as the energy harvester to power the whole tag, thus allowing its operation using any NFC-enabled smartphone.

## III. MATERIALS AND METHODS

### A. Flexible NFC Tag Design and Fabrication

The main electronic component of the NFC tag is an RFID chip model RF430FRL154H from Texas Instruments (Dallas, Texas, USA). This device is a 13.56-MHz transponder integrated circuit (IC) that embeds a programmable 16-bit MSP430 low-power microcontroller. The chosen chip is capable of harvesting energy from the electromagnetic (EM) field induced by an external NFC reader, thus allowing the development of a fully passive designs for portable and wireless sensing applications. To that end, an NFC antenna was designed (Fig. 2a) on the basis of the chosen transponder to operate at the frequency of 13.56 MHz. The NFC antenna consists of a squared planar inductor ($L_{ant}$) that couples with the inductor of the reader to induce current and allow the contactless energy transfer. To achieve resonance at 13.56 MHz, the inductance of the antenna was designed together with the internal capacitor ($C_{int}$) of the RF430FRL154H chip, which is placed in parallel with $L_{ant}$ to form a resonant LC circuit. In a parallel LC circuit, the resonance is achieved at $f_{res} = 1/(2\pi\sqrt{(LC)})$. Given that $C_{int} = 35$ pF at 13.56 MHz, the inductance value required for the resonance of the tag at $f_{res} = 13.56$ MHz was about $L_{ant} \sim 3.9\ \mu$H. However, to reduce the antenna dimensions, the inductance value was reduced at the expense of an increase in the capacitance value. On that basis, a 1.84 $\mu$H inductor was designed and an external capacitor of $C_{ext} = 40$ pF was placed in parallel to $C_{int}$. As a result, the equation of the resonance frequency in our parallel LC circuit was:

$$f_{res} = \frac{1}{2\pi\sqrt{L_{ant}(C_{int} + C_{ext})}} \tag{1}$$

To design the square-shaped planar spiral coil inductor, we have used the modified Wheeler formula as [70]:

$$L_{ant} = K_1 \mu_0 \frac{N^2 d}{1 + K_2 \rho} \tag{2}$$

where $\mu_0$ is the vacuum permeability ($4\pi \times 10^{-7}$ H/m); N is the number of turns;d is the average coil diameter calculated as $d = (d_{out} + d_{in})/2$; and $\rho$ is the filling ratio of the coil defined as $\rho = (d_{out} - d_{in}) / (d_{out} + d_{in})$. The parameters $K_1$ and $K_2$ are non-dimensional coefficients that depend on the antenna layout. For a square-shaped antenna, $K_1 = 2.34$ and $K_2 = 2.75$. The final designed antenna had N =7 turns and dimensions of 29 mm × 29 mm, with 500 $\mu$m as both the conductor width and the interspacing between the tracks. Using an RFID reader with an adequate electromagnetic (EM) field, the tag can generate a regulated voltage of ∼2 V with

an output current up to 500 $\mu$A. This is enough to power the LED indicator used in this work. As shown in the schematic diagram of Fig. 2(a), either the strain or the temperature sensor is connected in series with the LED indicator, thus modulating the LED light intensity as a function of the resistive variation in the sensor due to the strain or temperature. Such changes can give the user a visual semi-quantitative indication of the strain or temperature level, depending on the case.

Apart from the NFC chip and the external capacitor, some other passive components are required for the application circuit illustrated in Fig. 2(a). The circuit layout was designed using Altium Designer 19.1.7 (Altium Limited, NSW, Australia). The flexible printed circuit board (PCB) was fabricated using ultraviolet etching of flexible polyimide (PI) substrate having copper on one side and bonded together with a proprietary C-staged modified acrylic adhesive (AN210, C.I.F., Buc, France). The PI film had a thickness of 50 $\mu$m, a relative permittivity of $\varepsilon_r = 4.7$, and a loss tangent of $\tan\delta = 0.02$. The metallization layer was copper film with thickness of 35 $\mu$m and conductivity of $\sigma = 4.6 \times 10^7$ S/m. The EM simulations of the designed coil inductor along with the used materials (substrate and conductor) were carried out using Advanced Design Simulator (ADS, Keysight Technologies, Santa Clara, CA, USA). In these simulations, the high frequency and material effects (e.g., skin effect and substrate properties) were also considered. These were not included in previous calculations based on the Wheeler formula.

The tag was finally embedded in Polydimethylsiloxane (PDMS) to encapsulate and protect against moisture, liquid, etc., as shown in Fig. 2(c). PDMS is optically transparent through the visible spectrum, biocompatible, and resistant against chemicals such as water and the majority of alcohols and bases. The physical and chemical properties of PDMS make it well suited for packaging and encapsulation. For this work, Sylgard 184 PDMS (Dow Corning, U.S.) was supplied as a two-part component kit comprising of a base (part A) and a curing agent (part B). Both parts were mixed in a 10:1 ratio (A:B). The mixture was then degassed in a vacuum desiccator for 15 min in order to have a bubble-free mixture. After that, the mixture was poured into a rectangular mould ($7 \times 5$ cm$^2$), forming a thin layer of PDMS film. The tag was placed on top of the film after 20 min, allowing the mixture to be partially cured in room temperature conditions. Hence, the PDMS at this stage was uncured and the tag was embedded into the mixture. Afterwards, the filled mould was cured for 2 h at a relatively low temperature of 60 °C to prevent any damage to the electronic components. After curing, the sample was removed with a scalpel.

The antenna was characterized with the Precision Impedance Analyzer. Fig. 2(d) shows the frequency response of the fabricated planar loop before the RF430FRL154H chip was attached. The measured inductance (L) at 13.56 MHz was $1.808 \pm 0.003$ $\mu$H, which is very close to the designed value. The quality factor (Q) was higher than 75 at the frequency of interest, which is valid for this type of application. The self-resonance frequency was much higher than 13.56 MHz, close to 64 MHz in our case. Therefore, the coil can be

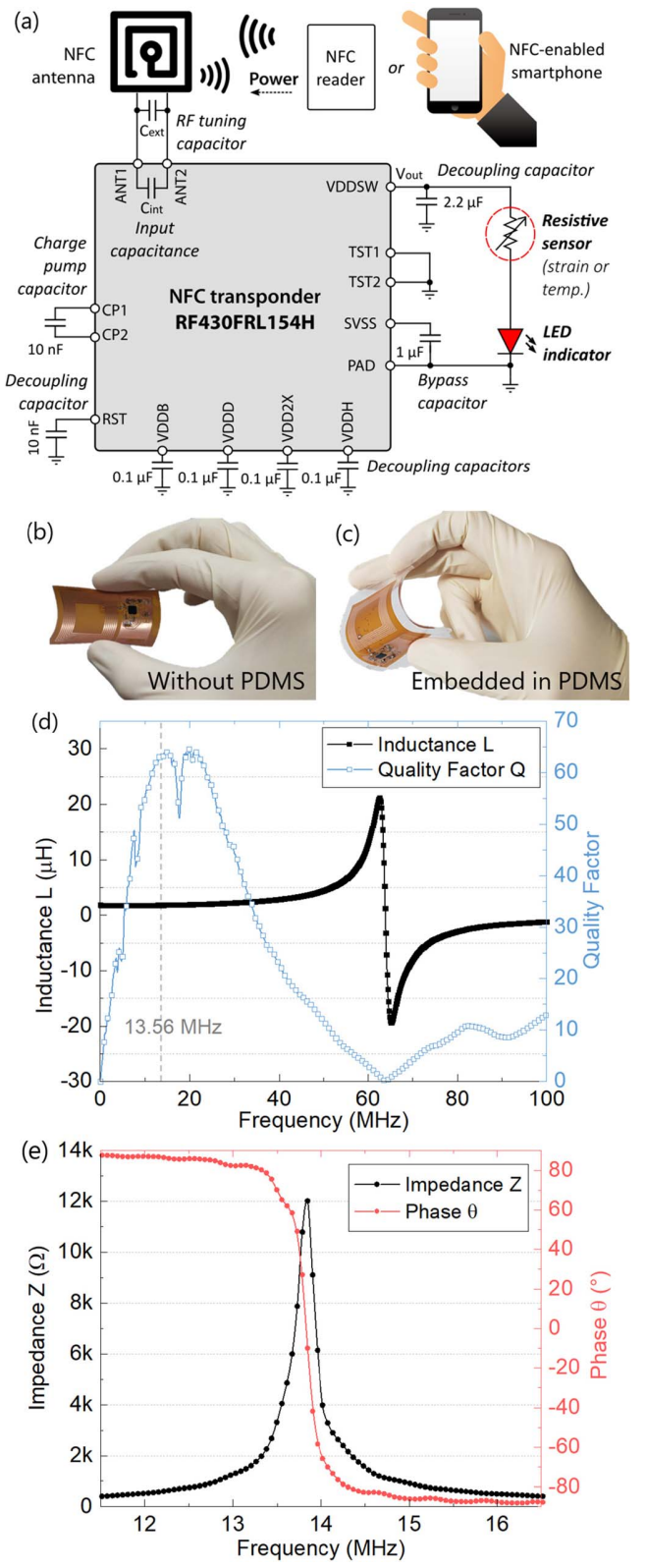


Fig. 2. (a) Schematic circuit diagram of the passive NFC tag for strain or temperature sensing. The sensor is connected in series with an LED indicator whose intensity is modulated according to the sensor value. (b-c) Photographs of the tag before and after embedding in PDMS. (d) Measured frequency response of the planar inductor in terms of inductance and quality factor; and (e) measured impedance and phase of the parallel LC circuit, which forms the antenna of the NFC tag.

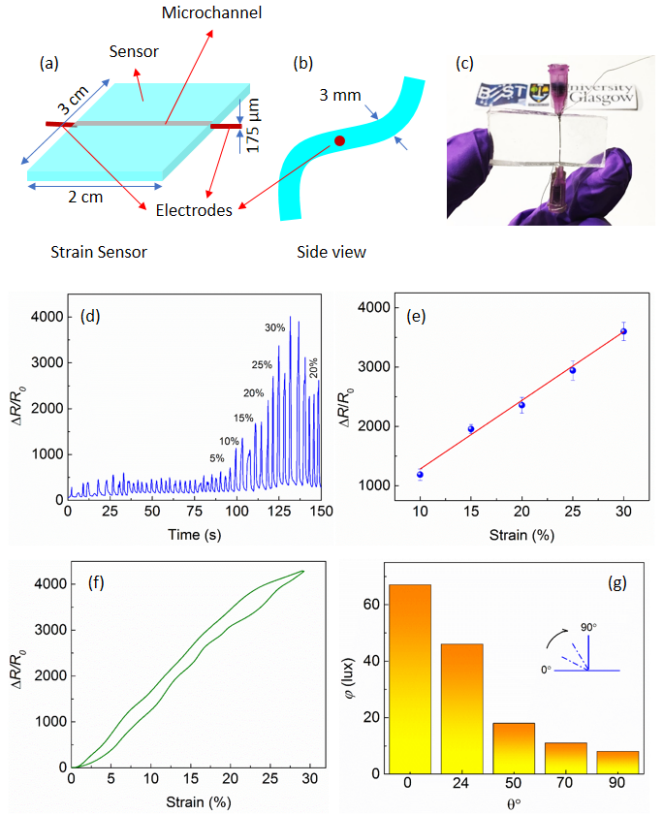


Fig. 3. (a, b) Schematic diagram of the fabricated strain sensor; (c) Optical image of the fabricated strain sensor; (d) Temporal response of the sensor for different amount of applied strain; (e) Strain sensor response with applied strain; (f) Hysteresis of the fabricated sensor for 30% applied strain; (g) The intensity of the LED ($\varphi$) with strain on the sensor due to different angle of bending ($\theta$).

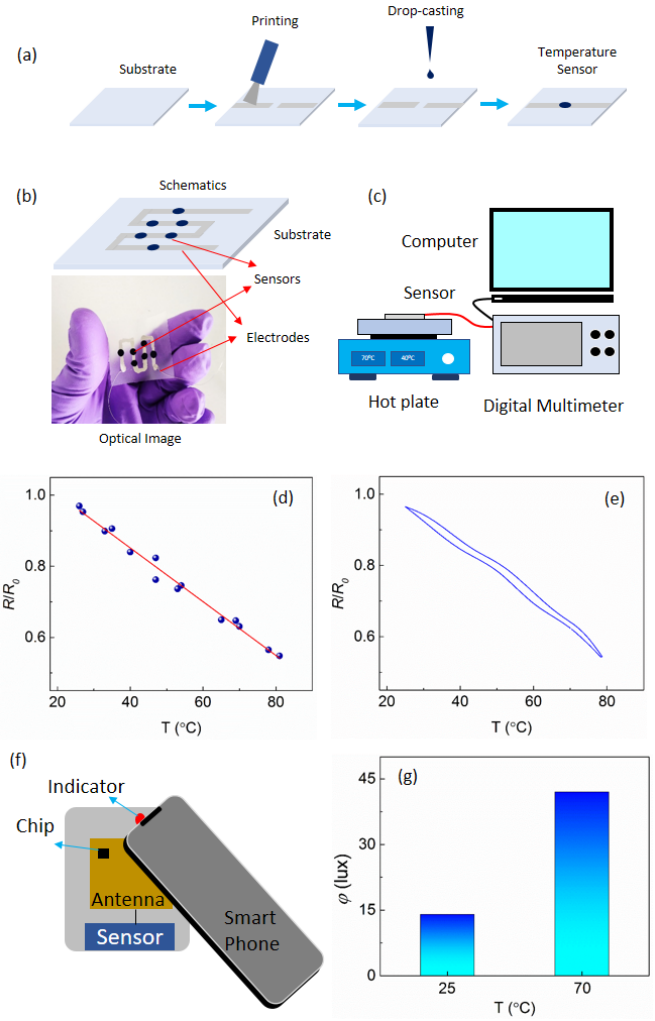


Fig. 4. (a) Fabrication steps for the temperature sensor; (b) Schematic and optical image of the fabricated temperature sensor for smart-packaging; (c) Schematic illustration of the experimental set-up for temperature sensor; (d) Temperature sensor response ($R/R_0$) with different temperature values; (e) Hysteresis of the fabricated sensor for 80°C temperature; (f) Schematic illustration of the temperature sensing system; (g) Optical intensity ($\varphi$) of LED due to different temperature (T).

considered valid for our requirements. After attaching the external capacitor and the chip to the flexible tag, the resonant circuit was completed. Therefore, a new frequency characterization was conducted measuring the impedance (Z) and phase ($\theta$) of the parallel LC resonant circuit, as depicted in Fig. 2(e), where we can observe the resonance peak close to the working frequency of 13.56 MHz.

### B. Strain Sensor Design and Fabrication

The PDMS and PEDOT:PSS materials were procured from Sigma Aldrich. Both materials were used for the development of the temperature and strain sensors. To fabricate the strain sensor, a 10:1 mixture of PDMS and cross-linker were made at room temperature. Thereafter, the mixture was poured into a circular mould (dia 5.5 cm) having a copper wire (dia ~180 $\mu$m) and degassed for 1 hr using a vacuum desiccator. The mould was then cured for 2 hrs at 60°C. The copper wire was then removed to fabricate the microchannel. A detailed manufacturing process is available in a previous work [14], [30]. Thereafter, conductive polymer PEDOT:PSS was injected into the microchannel and dried in a convection oven at 60°C for 1 hr. Afterwards, the electrodes were fixed using metal wires. The schematic diagram and the optical image of the fabricated sensor are shown in Fig. 3(a-c).

### C. Temperature Sensor Design and Fabrication

The temperature sensor was fabricated on a commercially available PVC substrate, which was procured from a local vendor. The conductive electrode was made of silver conductive paste (RS Components 186-3600, UK) using the stencil printing method. The conductive polymer PEDOT:PSS, procured from Sigma Aldrich, UK, was used as the temperature sensing material. Fig. 4(a) schematically illustrates the sensor fabrication steps on PVC substrate. Initially, 2 cm × 2 cm pieces of the PVC substrates were taken and two silver electrodes were printed on the PVC substrate with a gap of 2 mm, as illustrated in Fig. 4(a). The samples were then dried in a hot-air oven at 50 °C for 30 mins. After the drying process, a 10 $\mu$l of PEDOT:PSS was dispensed using a micro-pipette in the 2 mm gap. Thereafter, the samples were kept at 50 °C for 1 hr in an air-oven for drying. Then the samples were electrically characterised to evaluate their response. For the final tag design, a sensor array consisting

of 6 of such sensors were connected in series to increase the total resistance value, as illustrated in Fig. 4(b).

### D. Experimental Setup

The frequency characterization of the tag was carried out using an Agilent 4294A Precision Impedance Analyzer along with a 42941A impedance probe kit (Keysight Technologies, Santa Clara, CA, USA). A TRF7970A NFC/RFID Booster Pack from Texas Instruments was used as the RFID reader. Alternatively, the tag can also be operated with any NFC-enabled smartphone. A generic lux-meter mobile application was used for the characterization of the LED in terms of light intensity variation when the sensor's resistance changes due to the strain (e.g., bending) or temperature variation. Both sensors were characterized using a digital multimeter (Agilent 34461A) connected to a custom LabVIEW application. To characterize the strain sensor, a custom-made LabVIEW-enabled strain generation set-up was employed. This set up can apply uniaxial strain on the fabricated sensor by moving the two ends back and forth at different velocities. The two ends of the sensor were fixed on this set-up and electrical connections were taken out using thin metallic wires. A maximum of 30% strain was applied to the sensor. The sensor was characterized in terms of resistance as a function of the strain level.

Similarly, the temperature sensor was characterized using a temperature controllable hotplate (Stuart CD162). Fig. 4(c) shows the scheme of the experimental set-up. The sensor was placed on the hotplate and the electrodes were connected to a digital multimeter (Agilent 34461A) working with a custom LabVIEW application. The real-time temperature was monitored using a high-precision IR thermometer (FLUKE 62 MAX). The experiments were carried out in ambient conditions. The temperature of the hotplate was increased to the desired value and the sensor response (i.e., change in the resistance) was recorded. In all cases, the actual temperature was monitored using the IR thermometer.

## IV. Results and Discussion

### A. Strain Sensing

The fabricated resistive strain sensor showed an increase in the resistance value with the increase in the applied strain. Fig. 3(d) shows the temporal response of the sensor, i.e., the change in its normalized resistance ($R_N = (R - R_0)/R_0 = \Delta R/R_0$) over time for different strain conditions. Further, the strain percentage ($(\Delta L/L) \times 100\%$) was correlated with the normalized response ($R_N$) of the sensor, as depicted in Fig. 3(e). A maximum of 30% strain was applied to the sensor and the maximum recorded response was $\Delta R/R_0 \sim 4000$. The average gauge factor in this case is $\sim 13000$. Further, the hysteresis response was also studied, as shown in Fig. 3(f). The average degree of hysteresis (DH) was defined as $DH = (|A_L - A_U|/A_L) \times 100\%$, where $A_L$ and $A_U$ is the area under the loading and unloading curve, respectively. The DH value was in the range of $< 9\%$, which is considerably good.

The fabricated sensor was then connected to the NFC antenna and the LED as described previously. The sensor response was correlated with the intensity of the LED, which acted as a visual indicator. Upon introduction of the reader, the LED glowed and its intensity was related to the amount of strain experienced by the sensor. In this case, the NFC antenna was acting as the energy harvester for the whole tag. The change in the intensity of the LED was visible and distinguishable visually. However, for characterization purposes, the intensity of the light was measured using a lux-meter mobile application for the different strain conditions. As a semi-quantitative system, the presented solution is apt for large scale deployable packaging tags. Fig. 3(g) shows the light intensity of the LED connected in series to the sensor for different strain values. The intensity of the sensor decreased significantly when the sensor was in a bent condition, which could be the case for a faulty or inappropriate packaging. The brightness of the LED was highest ($\sim$67 Lux) for relaxed or no strain condition, whereas the intensity was significantly low ($\sim$8 Lux, causing the LED to be virtually off) for the highest strain condition. Fig. 3(g) also shows a decrease in the intensity of the LED brightness with the increase of the bending angle.

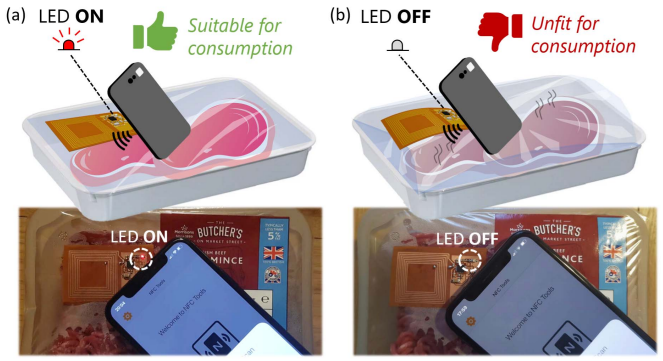


Fig. 5. Example of the application showing the NFC strain sensor tag attached to a food package for meat spoilage detection. The LED will be (a) ON if the product is suitable for consumption, or (b) OFF if the food is unfit for consumption due to Blown Pack Spoilage (BPS).

### B. Temperature Sensing

The conductive polymer PEDOT:PSS is also used here as the temperature sensing material. Upon a temperature increase, the mobility of the carriers inside the polymer is expected to increase, and hence the resistance should decrease. The single sensing element, prepared as discussed in Section III.C, was used for the electrical characterization. The sensor was connected to a LabVIEW enabled digital multimeter and placed on a hotplate having digital display control, as shown in Fig. 4(c). The temperature of the hotplate was varied from 25 to 90° C and the electrical response ($R/R_0$) was recorded for different temperatures. As expected, the resistance decreased with the increasing temperature, which is shown in Fig.4(d). The hysteresis of the sensor was also measured as shown in Fig. 4(e), where it can be observed that the average degree of hysteresis was $< \sim 3\%$. The schematic illustration of the temperature sensing system and the optical intensity response of the sensor are illustrated in Fig. 4(f-g), respectively.

### C. System Operation and Proof of Concept

As a proof of concept, the potential applicability of the proposed NFC-based strain sensor has been tested on a meat package for the detection of BPS, as illustrated in Fig. 5. For this purpose, it was first checked that the LED was ON with maximum brightness upon approach of an NFC-enabled smartphone when the meat was fresh and suitable for consumption (i.e., the package was not inflated). Afterwards, the meat package was kept in a non-refrigerated atmosphere to accelerate its spoilage. A few days later, the package started swelling due to the BPS effect. After the distention of the meat package caused by the spoilage, the LED did not turn on anymore upon approach of the reader smartphone to the tag, since the strain sensor resistance had increased upon bending (see Fig. 3), which indicated that the meat was unfit for consumption. This simple experiment illustrates the possibilities of the proposed sensing tag, thus opening new avenues in this field. While the simplicity of the resistive-based sensing mechanism does not provide a quantitative correlation between the sensor response and the exact spoilage status, the threshold detection is enough for the proposed application in the field of BPS. This simplicity allows, on the one hand, the use of any NFC-enabled smartphone as energy harvester without the need for an ad-hoc application. On the other hand, the NFC chip does not need to include any internal Analog to Digital Converter (ADC) module [71], making the design compatible with a wider range of commercially available NFC chips, which usually do not incorporate any type of Sensor Front End (SFE) interface [25], [72].

Similar to the strain sensing arrangement, the temperature sensor was also connected in series with the LED indicator. The associated circuit and system have been described in Fig. 2. Similar to the previous case, the NFC link acted as an energy harvester, i.e., the antenna was used to provide power to the tag upon approach of the reader. The resistance of the fabricated temperature sensor decreased with the increasing temperature. Hence, for a higher temperature, the optical intensity of the connected LED increases. In the presence of an NFC reader, the intensity of the LED varies depending on the temperature. This sensor in the tag also shows in a semi-quantitative way the temperature of any package. Fig. 4(f) schematically shows the sensing tag with a lux-meter mobile application, while Fig. 4(g) illustrates the intensity of the indicator at different temperatures. The intensity at 70°C was measured to be ∼42 lux whereas the intensity was ∼14 lux at room temperature (∼25°C).

## V. Conclusion

This paper presents a flexible strain sensor and a printed temperature sensor integrated with an NFC tag to detect the temperature and strain in a semi-quantitative and visual way. The resistive strain sensor was fabricated with a flexible polymer PDMS microchannel filled with conductive polymer PEDOT:PSS. It showed a maximum of three order increase in resistance for ∼100° bending. The PEDOT:PSS based temperature sensor showed a 70% change in resistance for a temperature change of ∼60°C. Each sensor was separately integrated with a custom-developed flexible NFC tag resonating at ∼13.56 MHz, which can be operated using any NFC-enabled smartphone. The strain or temperature level was obtained semi-quantitatively by means of the light intensity of a visual LED indicator connected with the antenna system. Finally, as a proof-of-concept, the paper showed how the presented wireless-enabled passive system can be used as a smart label for food packaging applications. It was shown how an NFC-based sensor system can allow a smartphone user to detect the food spoilage at an early stage. In the future, such systems could lead to automated decision-making, where the best course of action is automatically implemented with smart labels triggering an internet-connected device; for example, a robot in a supermarket.

## References


[1] H. Lim, H. S. Kim, R. Qazi, Y. Kwon, J. Jeong, and W. Yeo, "Advanced soft materials, sensor integrations, and applications of wearable flexible hybrid electronics in healthcare, energy, and environment," *Adv. Mater.*, vol. 32, no. 15, Apr. 2020, Art. no. 1901924, doi: 10.1002/adma.201901924.

[2] R. Dahiya, D. Akinwande, and J. S. Chang, "Flexible electronic skin: From humanoids to humans [scanning the issue]," *Proc. IEEE*, vol. 107, no. 10, pp. 2011–2015, Oct. 2019, doi: 10.1109/JPROC.2019.2941665.

[3] Y. Xiong, Y. Ge, L. Grimstad, and P. J. From, "An autonomous strawberry-harvesting robot: Design, development, integration, and field evaluation," *J. Field Robot.*, vol. 37, no. 2, pp. 202–224, Mar. 2020, doi: 10.1002/rob.21889.

[4] F. Bader and S. Rahimifard, "A methodology for the selection of industrial robots in food handling," *Innov. Food Sci. Emerg. Technol.*, vol. 64, Aug. 2020, Art. no. 102379, doi: 10.1016/j.ifset.2020.102379.

[5] R. Dahiya *et al.*, "Large-area soft e-skin: The challenges beyond sensor designs," *Proc. IEEE*, vol. 107, no. 10, pp. 2016–2033, Oct. 2019, doi: 10.1109/JPROC.2019.2941366.

[6] T. Q. Trung, S. Ramasundaram, B.-U. Hwang, and N.-E. Lee, "An all-elastomeric transparent and stretchable temperature sensor for body-attachable wearable electronics," *Adv. Mater.*, vol. 28, no. 3, pp. 502–509, 2016, doi: 10.1002/adma.201504441.

[7] M. D. Dankoco, G. Y. Tesfay, E. Benevent, and M. Bendahan, "Temperature sensor realized by inkjet printing process on flexible substrate," *Mater. Sci. Eng. B*, vol. 205, pp. 1–5, Mar. 2016, doi: 10.1016/j.mseb.2015.11.003.

[8] M. Soni, M. Bhattacharjee, M. Ntagios, and R. Dahiya, "Printed temperature sensor based on PEDOT: PSS-graphene oxide composite," *IEEE Sensors J.*, vol. 20, no. 14, pp. 7525–7531, Jul. 2020, doi: 10.1109/JSEN.2020.2969667.

[9] E. Hosseini, L. Manjakkal, D. Shakthivel, and R. Dahiya, "Glycine–chitosan-based flexible biodegradable piezoelectric pressure sensor," *ACS Appl. Mater. Interfaces*, vol. 12, no. 8, pp. 9008–9016, 2020, doi: 10.1021/acsami.9b21052.

[10] P. Escobedo, M. Ntagios, D. Shakthivel, W. T. Navaraj, and R. Dahiya, "Energy generating electronic skin with intrinsic tactile sensing without touch sensors," *IEEE Trans. Robot.*, vol. 37, no. 2, pp. 683–690, Apr. 2021, doi: 10.1109/TRO.2020.3031264.

[11] M. Ntagios, H. Nassar, A. Pullanchiyodan, W. T. Navaraj, and R. Dahiya, "Robotic hands with intrinsic tactile sensing via 3D printed soft pressure sensors," *Adv. Intell. Syst.*, vol. 2, no. 6, Jun. 2020, Art. no. 1900080, doi: 10.1002/aisy.201900080.

[12] D. Zymelka, T. Yamashita, S. Takamatsu, T. Itoh, and T. Kobayashi, "Printed strain sensor with temperature compensation and its evaluation with an example of applications in structural health monitoring," *Jpn. J. Appl. Phys.*, vol. 56, no. 5S2, 2017, Art. no. 05EC02, doi: 10.7567/JJAP.56.05EC02.

[13] P. K. Dubey, N. Yogeswaran, F. Liu, A. Vilouras, B. K. Kaushik, and R. Dahiya, "Monolayer $MoSe_2$-based tunneling field effect transistor for ultrasensitive strain sensing," *IEEE Trans. Electron Devices*, vol. 67, no. 5, pp. 2140–2146, May 2020, doi: 10.1109/TED.2020.2982732.

[14] M. Bhattacharjee, M. Soni, P. Escobedo, and R. Dahiya, "PEDOT:PSS microchannel-based highly sensitive stretchable strain sensor," *Adv. Electron. Mater.*, vol. 6, no. 8, Aug. 2020, Art. no. 2000445, doi: 10.1002/aelm.202000445.

[15] M. Bhattacharjee and D. Bandyopadhyay, "Mechanisms of humidity sensing on a CdS nanoparticle coated paper sensor," *Sens. Actuators A, Phys.*, vol. 285, pp. 241–247, Jan. 2019, doi: 10.1016/j.sna.2018.11.034.

[16] P. Escobedo *et al.*, "Compact readout system for chipless passive LC tags and its application for humidity monitoring," *Sens. Actuators A, Phys.*, vol. 280, pp. 287–294, Sep. 2018, doi: 10.1016/j.sna.2018.07.040.

[17] L. Manjakkal, S. Dervin, and R. Dahiya, "Flexible potentiometric pH sensors for wearable systems," *RSC Adv.*, vol. 10, no. 15, pp. 8594–8617, Feb. 2020, doi: 10.1039/D0RA00016G.

[18] L. Manjakkal, W. Dang, N. Yogeswaran, and R. Dahiya, "Textile-based potentiometric electrochemical pH sensor for wearable applications," *Biosensors*, vol. 9, no. 1, p. 14, 2019, doi: 10.3390/bios9010014.

[19] M. Bhattacharjee, A. Vilouras, and R. S. Dahiya, "Microdroplet-based organic vapour sensor on a disposable GO-chitosan flexible substrate," *IEEE Sensors J.*, vol. 20, no. 14, pp. 7494–7502, Jul. 2020, doi: 10.1109/JSEN.2020.2992087.

[20] A. Pullanchiyodan, L. Manjakkal, S. Dervin, D. Shakthivel, and R. Dahiya, "Metal coated conductive fabrics with graphite electrodes and biocompatible gel electrolyte for wearable supercapacitors," *Adv. Mater. Technol.*, vol. 5, no. 5, May 2020, Art. no. 1901107, doi: 10.1002/admt.201901107.

[21] K. B. Biji, C. N. Ravishankar, C. O. Mohan, and T. K. S. Gopal, "Smart packaging systems for food applications: A review," *J. Food Sci. Technol.*, vol. 52, no. 10, pp. 6125–6135, 2015, doi: 10.1007/s13197-015-1766-7.

[22] N. Zadbuke, S. Shahi, B. Gulecha, A. Padalkar, and M. Thube, "Recent trends and future of pharmaceutical packaging technology," *J. Pharmacy Bioallied Sci.*, vol. 5, no. 2, p. 98, 2013, doi: 10.4103/0975-7406.111820.

[23] M. Vanderroost, P. Ragaert, F. Devlieghere, and B. De Meulenaer, "Intelligent food packaging: The next generation," *Trends Food Sci. Technol.*, vol. 39, no. 1, pp. 47–62, Sep. 2014, doi: 10.1016/j.tifs.2014.06.009.

[24] L. Manjakkal, A. Pullanchiyodan, N. Yogeswaran, E. S. Hosseini, and R. Dahiya, "A wearable supercapacitor based on conductive PEDOT:PSS-coated cloth and a sweat electrolyte," *Adv. Mater.*, vol. 32, no. 24, Jun. 2020, Art. no. 1907254, doi: 10.1002/adma.201907254.

[25] A. Lazaro, R. Villarino, and D. Girbau, "A survey of NFC sensors based on energy harvesting for IoT applications," *Sensors*, vol. 18, no. 11, p. 3746, 2018, doi: 10.3390/s18113746.

[26] P. Kumar, H. W. Reinitz, J. Simunovic, K. P. Sandeep, and P. D. Franzon, "Overview of RFID technology and its applications in the food industry," *J. Food Sci.*, vol. 74, no. 8, pp. R101–R106, Oct. 2009, doi: 10.1111/j.1750-3841.2009.01323.x.

[27] P. Escobedo *et al.*, "Flexible passive near field communication tag for multigas sensing," *Anal. Chem.*, vol. 89, no. 3, pp. 1697–1703, 2017, doi: 10.1021/acs.analchem.6b03901.

[28] I. M. Perez de Vargas-Sansalvador, M. M. Erenas, A. Martínez-Olmos, F. Mirza-Montoro, D. Diamond, and L. F. Capitan-Vallvey, "Smartphone based meat freshness detection," *Talanta*, vol. 216, Aug. 2020, Art. no. 120985, doi: 10.1016/j.talanta.2020.120985.

[29] FAO, Rome, Italy. (2019). *The State of Food and Agriculture 2019. Moving Forward on Food Loss and Waste Reduction*. [Online]. Available: http://www.fao.org/3/ca6030en/ca6030en.pdf

[30] P. Escobedo, M. Bhattacharjee, F. Nikbakhtnasrabadi, and R. Dahiya, "Flexible strain sensor with NFC tag for food packaging," in *Proc. IEEE Int. Conf. Flexible Printable Sensors Syst. (FLEPS)*, Aug. 2020, pp. 1–4, doi: 10.1109/FLEPS49123.2020.9239568.

[31] P. E. Araque, I. M. P. de Vargas Sansalvador, N. L. Ruiz, M. M. Erenas, M. A. C. Rodriguez, and A. M. Olmos, "Non-invasive oxygen determination in intelligent packaging using a smartphone," *IEEE Sensors J.*, vol. 18, no. 11, pp. 4351–4357, Jun. 2018, doi: 10.1109/JSEN.2018.2824404.

[32] H. M. Húngaro, M. Y. R. Caturla, C. N. Horita, M. M. Furtado, and A. S. Sant'Ana, "Blown pack spoilage in vacuum-packaged meat: A review on clostridia as causative agents, sources, detection methods, contributing factors and mitigation strategies," *Trends Food Sci. Technol.*, vol. 52, pp. 123–138, Jun. 2016, doi: 10.1016/j.tifs.2016.04.010.

[33] B. Fletcher *et al.*, "Advances in meat spoilage detection: A short focus on rapid methods and technologies," *CyTA, J. Food*, vol. 16, no. 1, pp. 1037–1044, Jan. 2018, doi: 10.1080/19476337.2018.1525432.

[34] P. Zhang, P. Ward, L. M. Mcmullen, and X. Yang, "A case of 'blown pack' spoilage of vacuum-packaged pork likely associated with clostridium estertheticum in Canada," *Lett. Appl. Microbiol.*, vol. 70, no. 1, pp. 13–20, Jan. 2020, doi: 10.1111/lam.13236.

[35] K. Baldus and V. Deibel. Flavors Should Burst, Not Packages. Food-safety.com. Accessed: Jul. 29, 2021. [Online]. Available: https://www.food-safety.com/articles/3777-flavors-should-burst-not-packages

[36] W. H. Sperber and M. P. Doyle, *Compendium of the Microbiological Spoilage of Foods and Beverages*. New York, NY, USA: Springer, 2009.

[37] J. K. Brecht, S. A. Sargent, P. E. Brecht, J. Saenz, and L. Rodowick, "Protecting perishable foods during transport by truck and rail," in *USDA AMS Handbook*, vol. 669. Gainesville, FL, USA: Univ. of Florida, 2019.

[38] T. Tsironi, E. Dermesonlouoglou, M. Giannoglou, E. Gogou, G. Katsaros, and P. Taoukis, "Shelf-life prediction models for ready-to-eat fresh cut salads: Testing in real cold chain," *Int. J. Food Microbiol.*, vol. 240, pp. 131–140, Jan. 2017, doi: 10.1016/j.ijfoodmicro.2016.09.032.

[39] J. Wang, Z. Wen, B. Yang, and X. Yang, "Optical carbon dioxide sensor based on fluorescent capillary array," *Results Phys.*, vol. 7, pp. 323–326, Jan. 2017, doi: 10.1016/j.rinp.2016.12.044.

[40] L. Roberts, R. Lines, S. Reddy, and J. Hay, "Investigation of polyviologens as oxygen indicators in food packaging," *Sens. Actuators B, Chem.*, vol. 152, no. 1, pp. 63–67, Feb. 2011, doi: 10.1016/j.snb.2010.09.047.

[41] Y. Feng, L. Xie, Q. Chen, and L.-R. Zheng, "Low-cost printed chipless RFID humidity sensor tag for intelligent packaging," *IEEE Sensors J.*, vol. 15, no. 6, pp. 3201–3208, Jun. 2015, doi: 10.1109/JSEN.2014.2385154.

[42] J. Fernández-Salmerón, A. Rivadeneyra, M. A. C. Rodríguez, L. F. Capitan-Vallvey, and A. J. Palma, "HF RFID tag as humidity sensor: Two different approaches," *IEEE Sensors J.*, vol. 15, no. 10, pp. 5726–5733, Oct. 2015, doi: 10.1109/JSEN.2015.2447031.

[43] T. Tominaga, "Rapid detection of *Klebsiella pneumoniae, Klebsiella oxytoca, Raoultella ornithinolytica* and other related bacteria in food by lateral-flow test strip immunoassays," *J. Microbiol. Methods*, vol. 147, pp. 43–49, Apr. 2018, doi: 10.1016/j.mimet.2018.02.015.

[44] R. Lin *et al.*, "Wireless battery-free body sensor networks using near-field-enabled clothing," *Nature Commun.*, vol. 11, no. 1, p. 444, Dec. 2020, doi: 10.1038/s41467-020-14311-2.

[45] S. Ke *et al.*, "Screen-printed flexible strain sensors with Ag nanowires for intelligent and tamper-evident packaging applications," *Adv. Mater. Technol.*, vol. 5, no. 5, May 2020, Art. no. 1901097, doi: 10.1002/admt.201901097.

[46] T.-B. Nguyen, V.-T. Tran, and W.-Y. Chung, "Pressure measurement-based method for battery-free food monitoring powered by NFC energy harvesting," *Sci. Rep.*, vol. 9, no. 1, p. 17556, Dec. 2019, doi: 10.1038/s41598-019-53775-1.

[47] P. Müller and M. Schmid, "Intelligent packaging in the food sector: A brief overview," *Foods*, vol. 8, no. 1, p. 16, 2019, doi: 10.3390/foods8010016.

[48] C. J. Stannard, A. P. Williams, and P. A. Gibbs, "Temperature/growth relationships for psychrotrophic food-spoilage bacteria," *Food Microbiol.*, vol. 2, no. 2, pp. 115–122, 1985, doi: 10.1016/S0740-0020(85)80004-6.

[49] J. Heikenfeld *et al.*, "Wearable sensors: Modalities, challenges, and prospects," *Lab Chip*, vol. 18, no. 2, pp. 217–248, 2018, doi: 10.1039/c7lc00914c.

[50] R. S. Dahiya and M. Valle, *Robotic Tactile Sensing*. Dordrecht, The Netherlands: Springer, 2013.

[51] J. Hughes and F. Iida, "Multi-functional soft strain sensors for wearable physiological monitoring," *Sensors*, vol. 18, no. 11, p. 3822, 2018, doi: 10.3390/s18113822.

[52] D.-Y. Wang *et al.*, "High performance flexible strain sensor based on self-locked overlapping graphene sheets," *Nanoscale*, vol. 8, no. 48, pp. 20090–20095, 2016, doi: 10.1039/C6NR07620C.

[53] G. Rosati, M. Ravarotto, M. Scaramuzza, A. De Toni, and A. Paccagnella, "Silver nanoparticles inkjet-printed flexible biosensor for rapid label-free antibiotic detection in milk," *Sens. Actuators B, Chem.*, vol. 280, pp. 280–289, Feb. 2019, doi: 10.1016/j.snb.2018.09.084.

[54] L. Manjakkal, B. Sakthivel, N. Gopalakrishnan, and R. Dahiya, "Printed flexible electrochemical pH sensors based on CuO nanorods," *Sens. Actuators B, Chem.*, vol. 263, pp. 50–58, Jun. 2018, doi: 10.1016/j.snb.2018.02.092.

[55] Y. K. Kim, S.-H. Hwang, S. Kim, H. Park, and S. K. Lim, "ZnO nanostructure electrodeposited on flexible conductive fabric: A flexible photo-sensor," *Sens. Actuators B, Chem.*, vol. 240, pp. 1106–1113, Mar. 2017, doi: 10.1016/j.snb.2016.09.072.

[56] S.-J. Park, J. Kim, M. Chu, and M. Khine, "Highly flexible wrinkled carbon nanotube thin film strain sensor to monitor human movement," *Adv. Mater. Technol.*, vol. 1, no. 5, Aug. 2016, Art. no. 1600053, doi: 10.1002/admt.201600053.

[57] W. Navaraj and R. Dahiya, "Fingerprint-enhanced capacitive-piezoelectric flexible sensing skin to discriminate static and dynamic tactile stimuli," *Adv. Intell. Syst.*, vol. 1, no. 7, Nov. 2019, Art. no. 1900051, doi: 10.1002/aisy.201900051.
[58] L. Manjakkal, D. Shakthivel, and R. Dahiya, "Flexible printed reference electrodes for electrochemical applications," *Adv. Mater. Technol.*, vol. 3, no. 12, Dec. 2018, Art. no. 1800252, doi: 10.1002/admt.201800252.
[59] H. Niu and R. D. Lorenz, "Evaluating different implementations of online junction temperature sensing for switching power semiconductors," *IEEE Trans. Ind. Appl.*, vol. 53, no. 1, pp. 391–401, Jan. 2017, doi: 10.1109/TIA.2016.2614773.
[60] G. Liu *et al.*, "A flexible temperature sensor based on reduced graphene oxide for robot skin used in Internet of Things," *Sensors*, vol. 18, no. 5, p. 1400, 2018, doi: 10.3390/s18051400.
[61] Q. Liu, H. Tai, Z. Yuan, Y. Zhou, Y. Su, and Y. Jiang, "A high-performances flexible temperature sensor composed of polyethyleneimine/reduced graphene oxide bilayer for real-time monitoring," *Adv. Mater. Technol.*, vol. 4, no. 3, Mar. 2019, Art. no. 1800594, doi: 10.1002/admt.201800594.
[62] Y. Lu, M. C. Biswas, Z. Guo, J.-W. Jeon, and E. K. Wujcik, "Recent developments in bio-monitoring via advanced polymer nanocomposite-based wearable strain sensors," *Biosensors Bioelectron.*, vol. 123, pp. 167–177, Jan. 2019, doi: 10.1016/j.bios.2018.08.037.
[63] T. Vuorinen, J. Niittynen, T. Kankkunen, T. M. Kraft, and M. Mäntysalo, "Inkjet-printed graphene/PEDOT:PSS temperature sensors on a skin-conformable polyurethane substrate," *Sci. Rep.*, vol. 6, no. 1, 2016, Art. no. 35289, doi: 10.1038/srep35289.
[64] Y. Zhang and Y. Cui, "Development of flexible and wearable temperature sensors based on PEDOT:PSS," *IEEE Trans. Electron Devices*, vol. 66, no. 7, pp. 3129–3133, Jul. 2019, doi: 10.1109/TED.2019.2914301.
[65] P. Escobedo, M. Carvajal, L. Capitán-Vallvey, J. Fernández-Salmerón, A. Martínez-Olmos, and A. Palma, "Passive UHF RFID tag for multispectral assessment," *Sensors*, vol. 16, no. 7, p. 1085, Jul. 2016, doi: 10.3390/s16071085.
[66] Z. Cao *et al.*, "Near-field communication sensors," *Sensors*, vol. 19, no. 18, p. 3947, Sep. 2019, doi: 10.3390/s19183947.
[67] P. Escobedo *et al.*, "General-purpose passive wireless point–of–care platform based on smartphone," *Biosensors Bioelectron.*, vol. 141, Sep. 2019, Art. no. 111360, doi: 10.1016/j.bios.2019.111360.
[68] W. Dang, L. Manjakkal, W. T. Navaraj, L. Lorenzelli, V. Vinciguerra, and R. Dahiya, "Stretchable wireless system for sweat pH monitoring," *Biosensors Bioelectron.*, vol. 107, pp. 192–202, Jun. 2018, doi: 10.1016/j.bios.2018.02.025.
[69] P. Marsh *et al.*, "Flexible iridium oxide based pH sensor integrated with inductively coupled wireless transmission system for wearable applications," *IEEE Sensors J.*, vol. 20, no. 10, pp. 5130–5138, May 2020, doi: 10.1109/JSEN.2020.2970926.
[70] S. S. Mohan, M. D. M. Hershenson, S. P. Boyd, and T. H. Lee, "Simple accurate expressions for planar spiral inductances," *IEEE J. Solid-State Circuits*, vol. 34, no. 10, pp. 1419–1424, Oct. 1999, doi: 10.1109/4.792620.
[71] P. Escobedo, M. Bhattacharjee, F. Nikbakhtnasrabadi, and R. Dahiya, "Smart bandage with wireless strain and temperature sensors and batteryless NFC tag," *IEEE Internet Things J.*, vol. 8, no. 6, pp. 5093–5100, Mar. 2021, doi: 10.1109/JIOT.2020.3048282.
[72] M. Zurita, R. C. S. Freire, S. Tedjini, and S. A. Moshkalev, "A review of implementing ADC in RFID sensor," *J. Sensors*, vol. 2016, pp. 1–14, Jan. 2016, doi: 10.1155/2016/8952947.

**Pablo Escobedo** received the Major degrees in telecommunication engineering and electronics engineering, the master's degree in computer and network engineering, and the Ph.D. degree from the ECSens Group, Department of Electronics and Computer Technology, University of Granada (UGR), Spain, in 2012, 2013, 2014, and 2018, respectively. His Ph.D. thesis focused on the design and development of printed sensor systems on flexible substrates, with special interest in RFID/NFC technology. He is currently a Postdoctoral Research Fellow with the Bendable Electronics and Sensing Technologies (BEST) Group, University of Glasgow, U.K. His research interests include the development of printed smart labels for environmental, health and food quality monitoring applications, as well as eSkin for applications in the fields of robotics, prosthetics, health diagnostics, and wearables.

**Mitradip Bhattacharjee** (Member, IEEE) received the B.Tech. degree in electronics and communication engineering from the National Institute of Technology, India, in 2013, and the Ph.D. degree from Indian Institute of Technology, India, in December 2018. Subsequently, he joined the Bendable Electronics and Sensing Technologies (BEST) Research Group, University of Glasgow, U.K., as a Postdoctoral Fellow, in January 2019. He is currently an Assistant Professor with the Electrical Engineering and Computer Science Department, Indian Institute of Science Education and Research, Bhopal, India. His research interests include electronic sensors and systems, biomedical engineering, bioelectronics, flexible/printed and wearable electronics, wireless systems, and reconfigurable sensing antennas.

**Fatemeh Nikbakhtnasrabadi** (Graduate Student Member, IEEE) received the B.Sc. degree in electrical engineering and the M.Sc. degree in telecommunication engineering from Shahed University, Tehran, Iran, in 2010 and 2013, respectively. She is pursuing the Ph.D. degree with the Electronics and Nanoscale Division, Bendable Electronics and Sensing Technologies Group, University of Glasgow, U.K. Her current research interests include designing antennas and RFIDs for healthcare applications and smart labeling.

**Ravinder Dahiya** (Fellow, IEEE) is a Professor of Electronics and Nanoengineering with the University of Glasgow, U.K. He is also the Leader of the Bendable Electronics and Sensing Technologies (BEST) Research Group. His group conducts fundamental and applied research in the multidisciplinary fields of flexible and printable electronics, tactile sensing, electronic skin, robotics, and wearable systems. He has authored over 400 research articles, seven books, and submitted/granted 15 patents and disclosures. He has led several international projects. He holds the prestigious EPSRC Fellowship and received in past the Marie Curie Fellowship and Japanese Monbusho Fellowship. He has received several awards, including the 2016 Microelectronic Engineering Young Investigator Award and the 2016 Technical Achievement Award from the IEEE Sensors Council and ten best paper awards as author/coauthor. He was the Technical Program Co-Chair of IEEE SENSORS, in 2017 and 2018, respectively, and is the Founder of IEEE International Conference on Flexible Printable Sensors and Systems (FLEPS). He is the President-Elect (2020–2021) and a Distinguished Lecturer of the IEEE Sensors Council and is the Founding Editor-in-Chief of IEEE JOURNAL ON FLEXIBLE ELECTRONICS (J-Flex). He has served on the editorial boards of *Scientific Reports*, IEEE SENSORS JOURNAL, and IEEE TRANSACTIONS ON ROBOTICS.